JACS
JOURNAL OF THE AMERICAN CHEMICAL SOCIETY
Article
pubs.acs.org/JACS

Diruthenium–Polyyn-diyl–Diruthenium Wires: Electronic Coupling in the Long Distance Regime

Zhi Cao,[†,§] Bin Xi,[†,§] Diane S. Jodoin,[‡] Lei Zhang,[†] Steven P. Cummings,[†] Yang Gao,[†] Sarah F. Tyler,[†] Phillip E. Fanwick,[†] Robert J. Crutchley,*[,‡] and Tong Ren*[,†]

[†]Department of Chemistry, Purdue University, West Lafayette, Indiana 47907, United States
[‡]Department of Chemistry, Carleton University, Ottawa, Ontario K1S 5B6, Canada

Supporting Information

ABSTRACT: Reported herein is a series of $Ru_2(Xap)_4$ capped polyyn-diyl compounds, where Xap is either 2-anilinopyridinate (ap) or its aniline substituted derivatives. Symmetric $[Ru_2(Xap)_4](\mu\text{-}C_{4k})[Ru_2(Xap)_4]$ (compounds **4ka** (X = 3-isobutoxy) and **4kc** (X = 3,5-dimethoxy) with k = 2, 3, 4, and 5) was obtained from the Glaser coupling reaction of $Ru_2(Xap)_4(C_{2k}H)$. Unsymmetric $[Ru_2(Xap)_4](\mu\text{-}C_{4k+2})[Ru_2(ap)_4]$ (compounds **4k+2b** with k = 2, 3, and 4) were prepared from the Glaser coupling reaction between $Ru_2(Xap)_4(C_{2k+2}H)$ and $Ru_2(ap)_4(C_{2k}H)$. X-ray diffraction study of compound **12c** revealed both the sigmoidal topology of the polyyn-diyl bridge and the fine structural detail about the Ru_2 cores. Cyclic and differential pulse voltammetric (CV and DPV) measurements and spectroelectrochemical studies revealed that (i) the reduced monoanions $[Ru_2–C_{2m}–Ru_2]^{-1}$ (m = 4–8) belong to the Robin–Day class II mixed valent ions and (ii) the electronic coupling between Ru_2 termini depends on the length of the polyyn-diyl bridge with an attenuation constant (γ) between 0.12 and 0.15 $Å^{-1}$. In addition, spin-unrestricted DFT calculations provide insight about the nature of orbitals that mediate the long distance electronic coupling.

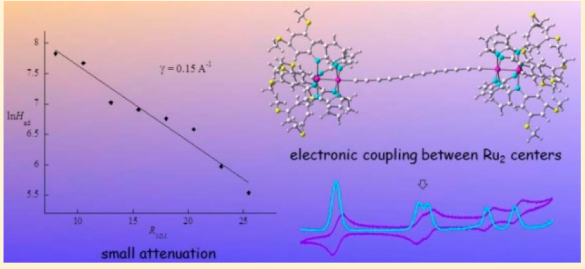

INTRODUCTION

Bimetallic compounds containing a polyyn-diyl bridge have fascinated both the organometallic and materials chemistry communities for decades. Earlier efforts during the 1960s–80s were focused on rigid rod oligomers/polymers, namely $[M–(C{\equiv}C)_m]_n$ with M as Ag, Au, Pd and Pt, with the hope that they might function as prototypical molecular wires,[1] and related compounds are still being pursued currently.[2] However, conductivity studies revealed that these compounds are instead insulators because of the electronic saturation of d^8 and d^{10} species.[3] Hence, the effort during the past two decades has been shifted to the bimetallic $[M]–(C{\equiv}C)_m–[M]$ type compounds based on the middle transition metals, and the degree of π-conjugation along the metal-polyyn-diyl backbone has been assessed using voltammetry, spectroelectrochemistry, and other techniques.[4,5] Noteworthy examples of $[M]–(C{\equiv}C)_m–[M]$ type compounds with significant electronic delocalization include those with [M] as CpFe(P–P),[6] CpRe(P)NO,[7,8] $CpRu(P)_2$,[9] (terpyridine)$Ru(P)_2$,[10] and $Mn(P–P)_2I$,[11] where P and P–P represent mono- and bidentate phosphines, respectively, and $Ru_2(DPhF)_4$ (DPhF = *N,N′*-diphenylformamidinate).[12] Though rare, trimetallic compounds with two bridging polyyn-diyls have been reported recently.[13] In addition to the interesting electronic properties of these compounds in bulk, recent years have seen several conductance studies of metal-alkynyl compounds at single or few molecule levels.[14]

There has been an intense interest in the mixed valency of dimeric and supramolecular assemblies based on metal–metal bonded dinuclear building blocks, and efforts from the laboratories of Cotton[15] and Chisholm[16] are noteworthy. Aiming at the discovery of new electronic and optoelectronic materials, our laboratory has investigated an array of diruthenium alkynyl compounds over the last 15 years.[5,17,18] In particular, a number of $[Ru_2(ap)_4](\mu\text{-}C_{2m})[Ru_2(ap)_4]$ type compounds (ap = 2-anilinopyridinate, m = 1–4, and 6) were prepared and thoroughly characterized,[19,20] where the facile electron transfers between two $[Ru_2]$ termini mediated by polyyn-diyl chains were demonstrated based on voltammetric and spectroelectrochemical measurements. It has been our interest to explore the same type of structure–property relationship at longer distances. Several obstacles confronted this effort: the inherent instability of species containing extended polyyne chains, poor solubility of $[Ru_2(ap)_4]_2(\mu\text{-}C_{2m})$ and the difficulty of accessing species with odd number of C≡C units, namely $[Ru_2]_2(\mu\text{-}C_{4k+2})$. In this contribution, we report the detailed syntheses, spectroscopic and voltammetric studies of a more soluble series of symmetric $[Ru_2(Xap)_4]_2(\mu\text{-}C_{4k})$ (k = 2, 3, 4, and 5) and unsymmetric $[Ru_2(Xap)_4](\mu\text{-}C_{4k+2})[Ru_2(ap)_4]$ (k = 2, 3, and 4) compounds with Xap = 2-(3,5-dimethoxyanilino)pyridinate (DiMeOap)[21] and 2-(3-isobutoxyanilino)pyridinate (^{i}BuOap),[22] as defined in Chart 1. Spin-unrestricted DFT calculations on two model compounds based on **10b** and **12c**, the structural characterizations

Received: July 14, 2014
Published: August 12, 2014

   dx.doi.org/10.1021/ja507107t | J. Am. Chem. Soc. 2014, 136, 12174–12183

Chart 1. Ru_2–Polyyn–Ru_2 Studied Herein

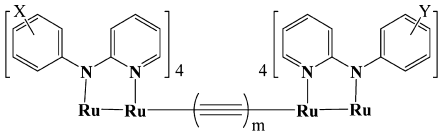

2ma: X = Y = 3-isobutoxy
2mb: X = 3-isobutoxy; Y = H
2mc: X = Y = 3,5-dimethoxy

on **12c**, and the spectroelectrochemical studies of the mixed-valence monoanions of **8a**–**16a** are also reported herein.

RESULTS AND DISCUSSION

Synthesis. Few families of extended polyyn-diyl bridged bimetallic compounds have been systematically investigated and include those based on $CpRe(PPh_3)NO$,[8] *trans*-(*p*-tolyl)(*p*-$tol_3P)_2Pt$[23,24] and Cp*Ru(dppe).[25] In the case of Re species, the Re–$(C{\equiv}C)_kR$ precursors with $k \geq 3$ were prepared from the Cadiot–Chodkiewicz reaction, and the dirhenium species were prepared from the Glaser reaction.[8] With the (*p*-tolyl)$Pt(P(p\text{-tolyl})_3)_2$ capping unit, the Pt–$(C{\equiv}C)_kR$ precursors with $k \geq 3$ were prepared from Pt–$(C{\equiv}C)_2H$ using the Glaser reaction, and subsequently homodimerized to yield Pt–$(C{\equiv}C)_{2k}$–Pt with k as high as 7.[23,24] The diplatinum species Pt–$(C{\equiv}C)_m$–Pt with m being odd were prepared from the reaction between Pt–$(C{\equiv}C)_m$H and Cl–Pt in the presence of $CuI/HNEt_2$.[24] A fairly unique approach has been developed for the preparation of [Ru]–$(C{\equiv}C)_{x+y}$–[Ru] ([Ru] = Cp*Ru(dppe)): a Cadiot–Chodkiewicz like reaction between [Ru]–$(C{\equiv}C)_x$–$Au(PPh_3)$ and I–$(C{\equiv}C)_yY$ resulted in either the polyyne extension (Y = silyl) or the dimerization (Y = I).[25,26]

The monopolyynyl $Ru_2(Xap)_4$ precursors can be prepared from metathesis reactions between $Ru_2(Xap)_4Cl$ and $LiC_{2k}SiMe_3$ in satisfactory yields when the polyyne is short (k = 1–3).[21,22,27] The monomers $Ru_2(Xap)_4(C_8SiEt_3)$ and $Ru_2(Xap)_4(C_{10}SiEt_3)$ may be prepared from either the Glaser oxidative coupling reaction under Hay conditions[28] or the Cadiot–Chodkiewicz coupling reaction.[29] While the former method found success in our earlier work in producing related compounds,[30] it has the drawback of producing a substantial amount of homocoupled byproducts and hence was not used in this work. Encouraged by the aforementioned successes in preparing Pt-polyyynyl[23] and Re-polyyynyl,[31] the Cadiot–Chodkiewicz coupling method was adopted for the preparation of longer $Ru_2(Xap)_4(C_{2k}SiR_3)$. As shown in Scheme 1, the reaction between $Ru_2(Xap)_4(C_6H)$ and $BrC{\equiv}CSiEt_3$ yielded the compound $Ru_2(Xap)_4(C_8SiEt_3)$, which was subsequently converted to the compound $Ru_2(Xap)_4(C_8H)$ using K_2CO_3. The further extended $Ru_2(Xap)_4(C_{10}H)$ was prepared in the same fashion from $Ru_2(Xap)_4(C_8H)$. Due to the slow degradation of both $Ru_2(Xap)_4(C_8H)$ and $Ru_2(Xap)_4(C_{10}H)$ under ambient conditions, they were prepared *in situ* from $Ru_2(Xap)_4(C_8SiEt_3)$ and $Ru_2(Xap)_4(C_{10}SiEt_3)$ and subjected to further reactions immediately.

Scheme 1. Syntheses of Extended Mono-Ru_2 Polyyynyl[a]

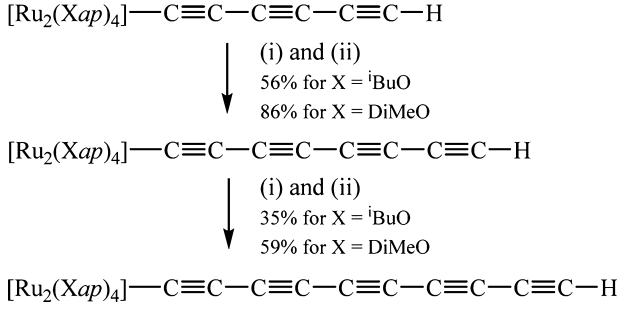

[a]Conditions: (i) BrC_2SiEt_3, *n*-BuLi, CuI, Et_2NH and (ii) K_2CO_3, THF/MeOH; X = ^{t}BuO, DiMeO, or nothing.

The symmetrically bridged compounds $[Ru_2(Xap)_4]_2(\mu\text{-}C_{4k})$ (**4ka** and **4kc** with k = 2, 3, 4, and 5) were prepared through the Glaser coupling reaction of the corresponding $Ru_2(Xap)_4(C_{2k}H)$ monomers as shown in Scheme 2. Similarly,

Scheme 2. Syntheses of Ru_2–Ru_2 Polyyn-diyl Complexes with Even and Odd Numbers of C–C Bonds[a]

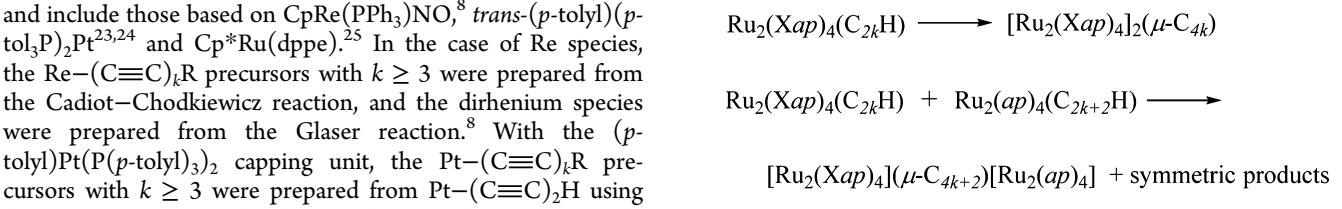

[a]Condition for procedures: cat. CuCl/TMEDA, O_2, acetone; Yields: symmetric dimers, **8a**, 71%; **12a**, 62%; **16a**, 56%; **20a**, 32%; unsymmetric dimers, **10b**, 34%; **14b**, 28%; **18b**, 14%.

the unsymmetric compounds $[Ru_2(^tBuOap)_4](\mu\text{-}C_{4k+2})$-$[Ru_2(ap)_4]$ (**4k+2b**, k = 2, 3, and 4) were synthesized by the coupling reactions of the mixture containing two different monomers, $Ru_2(^tBuOap)_4(C_{2k+2}H)$ and $Ru_2(ap)_4(C_{2k}H)$, as shown in Scheme 2. Both types of coupling reactions were performed under the Hay conditions to provide symmetric or unsymmetric products in moderate to good yields. Symmetric compounds $[Ru_2(Xap)_4]_2(\mu\text{-}C_{4k+4})$ and $[Ru_2(ap)_4]_2(\mu\text{-}C_{4k})$ were present as byproducts from the coupling reaction of mixed monomers, and they were successfully isolated by preparative TLC. Both the $Ru_2(Xap)_4(C_{2k}H)$ monomers and the bridged compounds are paramagnetic and cannot be unambiguously characterized with ^{1}H NMR spectroscopy. Instead, these compounds were authenticated by HR-*n*ESI-MS and single-crystal X-ray diffraction study (**12c**).

Molecular Structure. Previously reported $[Ru_2(Xap)_4]_2(\mu\text{-}C_{2m})$ type structures include m = 2 and 4 with $Ru_2(ap)_4$ and m = 3 with $Ru_2(DiMeOap)_4$.[18,20] With the more soluble DiMeOap ligand, X-ray quality crystals of compound **12c** were obtained. The structural plot of **12c** is shown in Figure 1, and the selected metric parameters are also provided in the caption. Compound **12c** exhibits a sigmoidal Ru_2–C_{12}–Ru_2 backbone and contains a crystallographic inversion center that bisects the C_{12} chain. Similar *S*-shape M–C_x–M geometries have been observed in the structures of Pt–C_{10}–Pt and Pt–C_{12}–Pt[24] and Ru–C_{14}–Ru.[25] From Figure 1, it is evident that the coordination environments of the Ru_2 cores in **12c** are very similar to those observed in the previous studies of $Ru_2(Xap)_4$–alkynyl complexes.[5] DiMeOap ligands adopt the (4,0) arrangement with all anilino N-centers coordinated to one Ru center (4 site) and all pyridine N-centers coordinated to the other Ru center (0 site). The Ru–Ru bond length in **12c** (2.366(1) Å) is slightly elongated from those found for other $[Ru_2(Xap)_4]_2(\mu\text{-}C_{2m})$ (2.324–2.331 Å, m = 2 and 3).[18,20] The elongation is likely due to a strong Ru–C bond in **12c**, which in turn is attributed to the electron deficiency of the C_{12} chain.

dx.doi.org/10.1021/ja507107t | J. Am. Chem. Soc. 2014, 136, 12174–12183

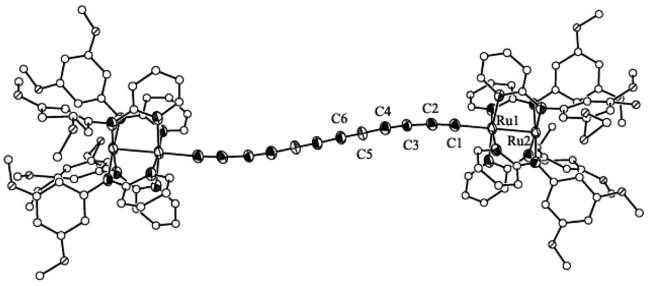

Figure 1. Structural plot of compound **12c**, hydrogen atoms are omitted for clarity. Selected bond lengths (Å) and angles (deg): Ru1 − Ru2, 2.366 (1); Ru1 − C1, 2.03 (1); Ru1 − N11, 2.072(7); Ru1 − N31, 2.068(8); Ru1 − N51, 2.084(8); Ru1 − N71, 2.055(8); Ru2 − N2, 2.021(7); Ru2 − N4, 2.031(8); Ru2 − N6, 2.018(7); Ru2 − N8, 2.025(8); C1 − C2, 1.24(1); C2 − C3, 1.38(1); C3 − C4, 1.21(1); C4 − C5, 1.33(1); C5 − C6, 1.24(1); C6 − C6A, 1.36(2); C1 − Ru1 − Ru2, 179.0(3); C2 − C1 − Ru1, 175.2(9); N(av.) − Ru1 − Ru2, 87.1(2); N(av.) − Ru2 − Ru1, 88.5(6); C1 − C2 − C3, 173.4(11); C2 − C3− C4, 173.9(11); C3 − C4 − C5, 174.3(11); C4 − C5− C6, 176.4(12).

Voltammetric Properties. Rich redox characteristics have been the hallmark of both the $Ru_2(Xap)_4(C_{2k}SiR_3)$ and $[Ru_2(Xap)_4]_2(\mu\text{-}C_{2m})$ type compounds.[5] $Ru_2(Xap)_4(C_{2k}SiR_3)$ (k = 2, 3, 4, and 5) species reported herein generally exhibit two reversible one-electron processes localized on the Ru_2 center: a reduction (**A**) between −0.45 and −0.55 V and an oxidation between 0.55 and 0.70 V (**B**), as illustrated by the voltammograms of $Ru_2(^{i}BuOap)_4$ type compounds provided in the Supporting Information. It is noted that the $E_{1/2}$ for both couples **A** and **B** anodically shift as k increases, reflecting the increase in the electron-deficiency of $-C_{2k}SiR_3$ with increasing k.

Both the cyclic (CV) and differential pulse (DPV) voltammograms of symmetric compounds **8a**, **12a**, **16a**, and **20a**, and unsymmetric compounds **10b**, **14b**, and **18b** are shown in Figure 2, while the potential data and K_C (comproportionation constants, see discussion below) for the monoanions are listed in Table 1. The voltammograms and potential data for compounds **8c**−**20c** are provided in the Supporting Information. All compounds display two pairs of one-electron reductions between −0.34 and −2.01 V. The less cathodic pair is attributed to the reductions of the Ru_2 centers that is related to the 1e$^-$ reduction (**A**) of $Ru_2(Xap)_4(C_{2k}SiR_3)$. The more cathodic pair is likely due to reduction of the polyyn-diyl bridge. The stepwise appearance rather than a 2e$^-$ wave is indicative of significant electronic coupling between two $[Ru_2]$ termini.[32] In the anodic region, all compounds studied herein undergo a pseudo two-electron wave between 0.54 and 0.59 V, while pairwise one electron waves were observed for $[Ru_2(Xap)_4]_2(\mu\text{-}C_{2m})$ compounds with m = 1−3.[18,20] The pseudo two-electron waves in compounds of $m \geq 4$ are the result of coalescence of two one-electron waves observed for compounds of m = 1−3 because of the gradually weakening $Ru_2\cdots Ru_2$ coupling as the polyyn-diyl chain elongates. It is clear from Table 1 that the $\Delta E(-1)$ (= $E_{1/2}(0/-1) - E_{1/2}(-1/-2)$) gradually decreases as m increases, again reflecting the inverse dependence of electronic coupling on $Ru_2\cdots Ru_2$ separation.[33] In general, potentials for all redox couples display a significant anodic shift as the polyyne chain elongates, which is attributed to the electron-deficient nature of the added acetylene units.

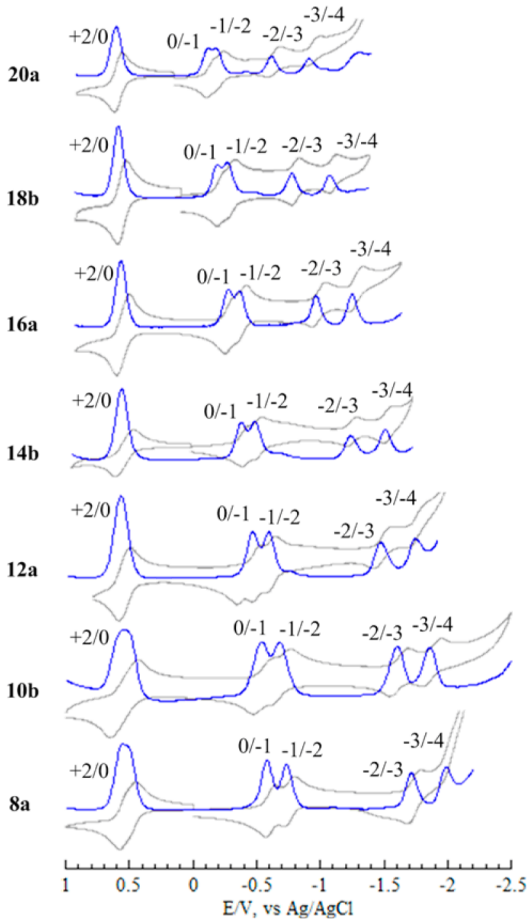

Figure 2. Cyclic and differential pulse voltammograms of compounds **8a**, **10b**, **12a**, **14b**, **16a**, **18b**, and **20a** recorded in 0.2 M THF solution of Bu_4NPF_6.

Table 1. Electrochemical Data from DPV Studies (vs Ag/AgCl) and Comproportionation Constant for Monoanionic Species

molecule	+2/0	0/−1	−1/−2	−2/−3	−3/−4
8a	0.54	−0.61	−0.77	−1.74	−2.01
			$K_C(-1)$ =456		
10b	0.55	−0.54	−0.68	−1.60	−1.86
			$K_C(-1)$ =212		
12a	0.58	−0.46	−0.59	−1.46	−1.74
			$K_C(-1)$ =129		
14b	0.58	−0.42	−0.54	−1.33	−1.62
			$K_C(-1)$ = 89		
16a	0.58	−0.41	−0.51	−1.22	−1.55
			$K_C(-1)$ = 47		
18b	0.58	−0.38	−0.47	−1.10	−1.46
			$K_C(-1)$ = 41		
20a	0.59	−0.34	−0.43	−0.99	−1.38
			$K_C(-1)$ = 37		

Among the related M−C_{2m}−M type compounds, the series with M = CpRe(P)NO termini exhibits well-defined stepwise reversible 1e$^-$ oxidations with m up to 4, and irreversible 1e$^-$ oxidations thereafter (m = 5, 6, and 8).[8] The series with M = Cp*Ru(dppe) exhibits well-defined stepwise (quasi)reversible 1e$^-$ oxidations with m up to 8.[25] The series with M = (Aryl)Pt(P)$_2$ does not display stepwise redox couples at

dx.doi.org/10.1021/ja507107t | J. Am. Chem. Soc. 2014, 136, 12174−12183

all.[23,24,34] The series reported herein is unique in exhibiting stepwise 1e$^-$ reductions, a feature that sustains with m up to 10.

Electronic Spectroscopy. The $Ru_2(Xap)_4(C_{2k}R)$ monomers based on both ^{i}BuOap and DiMeOap ligands generally display two intense bands in the Vis-NIR region similar to the previously studied $Ru_2(ap)_4(C_{2k}R)$ type compounds.[5,22] The spectra of $Ru_2(^i BuOap)_4(C_{2k}R)$ with k up to 5 are provided in Supporting Information. According to a TD-DFT analysis previously published by our laboratory,[22] the low-energy band at ca. 760 nm is assigned as the transitions to the $\delta^*(Ru_2)$ orbital from both the Ru−N(Xap) and π(Ru−Ru) orbitals, which have a minimum dependence on the length of polyynyl. The high-energy band at ca. 490 nm is attributed to the transitions to the $\delta^*(Ru_2)$ orbital from both the π(C≡C) orbitals (predominant) and Ru−N(Xap) orbitals (minor) and exhibits blue shift as the polyynyl chain elongates.

The vis−NIR spectra of compounds **8a**, **10b**, **12a**, **14b**, and **16a** are shown in Figure 3. Upon the formation of bridged

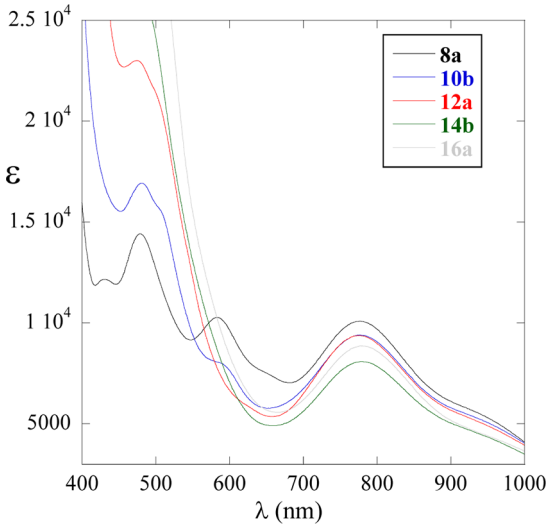

Figure 3. Vis-NIR spectra of (μ-C_{2m}) compounds (m = 4−8) based on the ^{i}BuOap ligand recorded in THF.

dimers, the absorption spectra become both intensified and more complex compared with the corresponding $Ru_2(^i BuOap)_4(C_{2k}R)$ precursors. In the previous report of $[Ru_2(ap)_4]_2(\mu$-$C_{2m})$ (m = 1−3),[20] the spectra clearly featured four major transitions: a shoulder at ca. 450 nm, a very intense peak at ca. 570 nm, another intense peak centered at 750 nm, and a peak (shoulder) around 890 nm. As the polyyn-diyl chain elongates, the intensities for both the peak at 590 nm and the shoulder at ca. 950 nm gradually diminish. Specifically, the peak at ca. 590 nm is still distinct in **8a** and **10b** but completely disappears with $m \geq 6$. From **8a** to **16a**, the shoulder at ca. 950 nm remains observable with decreasing intensity as n increases. Similar to the $Ru_2(Xap)_4(C_{2k}R)$ monomers, the intense absorption at 470 nm is associated with the π(C≡C) → $\delta^*(Ru_2)$ transition and is consequently sensitive toward the degree of π delocalization in the polyyn-diyl backbone. In fact, the intensity increased nearly 3-fold from **8a** to **16a**. Originating from the Ru−N(Xap) and π(Ru−Ru) to δ^*(Ru−Ru) transitions, the peak centered at 780 nm has a weak dependence on the length of polyyn-diyl since π(C≡C) orbitals are not directly involved in either the ground state or the excited state.

Spectroelectrochemistry. Spectroelectrochemical reductions of **8a**, **10b**, **12a**, **14b**, **16a**, **18b**, and **20a** were performed and a representative study for **8a** is shown in Figure 4, while

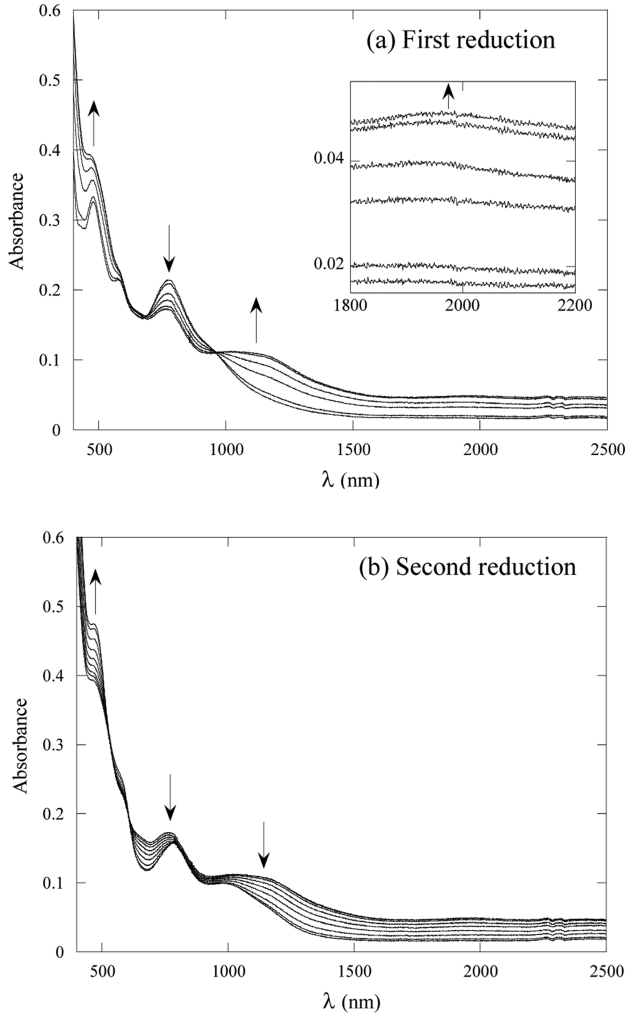

Figure 4. First (a) and second (b) spectroelectrochemical reductions of **8a** in THF solution; the IVCT band at 2120 nm is shown in the inset of (a).

those of **10b**, **12a**, **14b**, and **16a** have been placed in Supporting Information. Compounds **18b** and **20a** were unstable in solution, and their spectroelectrochemistry was not investigated.

Reduction of **8a** shows growth of two new bands at 1140 and 2120 nm (Figure 4a, the λ_{max}s are derived from the spectral deconvolution discussed below). These bands are not present for the doubly reduced species (Figure 4b) and are therefore assigned to intervalence transitions (IT). Similar IT bands of greater intensity have been previously reported for $[Ru_2(ap)_4]_2(\mu$-$C_4)$ and $[Ru_2(^i BuOap)_4]_2(\mu$-$C_6)$ compounds.[18,20] It is possible to deconvolute these IT bands from the absorption envelope assuming Gaussian band shape, and the results of this deconvolution for $(\mathbf{8a})^{1-}$−$(\mathbf{16a})^{1-}$ compounds have been compiled in Table 2. Figures of the Gaussian band fitting have been placed in Supporting Information.

The proximity of the high-energy intervalence band (IT_2) to the more intense band at 850 nm is problematic to the fitting process because the intensity of the 850 nm band varies with

dx.doi.org/10.1021/ja507107t | J. Am. Chem. Soc. 2014, 136, 12174−12183

Table 2. Deconvoluted Intervalence Band Data of the $(8a)^{1-}-(16a)^{1-}$ Compounds[a]

	IT_1			IT_2		
compound	ν	$\nu_{1/2}$	ε_{max}	ν	$\nu_{1/2}$	ε_{max}
8a	4710	5430	1860	8780	2710	4080
10b	5737	3956	1410	8454	2313	2380
12a	5470	4420	1840	9050	2610	4220
14b	5950	4150	680	9370	2690	3200
16a	5360	4670	1090	8940	2140	4670
6a[b]	5180	2020	7360			
4[b]	5670	1630	7700			

[a]All data in cm^{-1} except for ε_{max} in M^{-1} cm^{-1}. [b]Taken from refs 18 and 20, and **4** is based on $Ru_2(ap)_4$.

the length of the bridge. The low-energy intervalence band (IT_1) is sufficiently removed from this interference so that its spectral data are more reliable.

The successful preparation of polyyn-diyl (C_{2m}) bridged dimers with m up to 10 offers the possibility of probing electronic coupling over a tunable distance. As shown in Table 1, the comproportionation constant decreases steadily as the separation between bridged metal centers increases, and this suggests a concomitant decrease in metal−metal coupling. However, the free energy of comproportionation is made up of a number of free energy terms as shown below.[35]

$$\Delta G_c = \Delta G_s + \Delta G_e + \Delta G_i + \Delta G_r + \Delta G_{ip} \quad (1)$$

In eq 1, ΔG_s reflects the statistical distribution of the comproportionation equilibrium, ΔG_e accounts for the electrostatic repulsion of two like-charged metal centers, ΔG_i is an inductive factor dealing with competitive coordination of the bridging ligand by the metal ions, ΔG_r is the free energy associated with the stabilizing effect of metal−metal coupling on the mixed-valence ions, and ΔG_{ip} is the difference in ion pairing between redox products. For the reduction of neutral compounds in low-dielectric solvents, ΔG_{ip} can be significant and is of opposite sign compared to the other factors in eq 1 and so decreases ΔG_c. Our cyclic voltammetry studies used 0.2 M Bu_4NPF_6 as electrolyte, and it is expected that ion pairing between Bu_4N^+ and **8a**−**20a** anions will be small. Furthermore, if we make the assumption that for $[\mathbf{8a}]^{2-}-[\mathbf{20a}]^{2-}$ the anion centers are sufficiently separated so that ion pairing effects are the same as for $[\mathbf{8a}]^{1-}-[\mathbf{20a}]^{1-}$, $\Delta G_{ip} \approx 0$ and can be ignored. The other nonresonance exchange contributions to the free energy of comproportionation $\Delta G_{nr} = \Delta G_s + \Delta G_e + \Delta G_i$ are also expected to be small under the conditions of our study and can be best estimated by the ΔG_c of the weakest coupled system, **20a** (Table 3), ΔG_{nr} = 90 mV. The difference between ΔG_c and ΔG_{nr} would thus be a measure of ΔG_r, which, because there are two mixed-valence complexes generated in the comproportionation equilibrium, should be divided by a factor of 2, yielding $\Delta G_r'$, the free energy resonance exchange for a single mixed-valence complex. Values of $\Delta G_r'$ for the compounds of this study as well as those of previously reported data for **4**[20] and **6a**[18] have been placed in Table 3.

Anions $[\mathbf{8a}]^{1-}-[\mathbf{20a}]^{1-}$ are Class II mixed-valence complexes, and the free energy of resonance exchange can be related to the resonance exchange integral H_{ad} according to eq 2:[36]

Table 3. Estimates of Bridged Ruthenium Ion Separation, the Free Energy Comproportionation, the Free Energy Resonance Exchange, and Resonance Exchange Coupling Element

compound	R_{MM} (Å)[a]	ΔG_c (mV)[b]	$\Delta G_r'$ (mV)[c]	H_{ad}[d] (cm^{-1})	H_{ad}[e] (cm^{-1})
4[f]	8	380	145	2510	687
6a[g]	10.5	200	105	2140	544
8a	13	157	33	1200	380
10b	15.5	137	23	1000	181
12a	18	124	17	860	177
14b	20.5	114	12	720	95
16a	23	97	3.5	390	88
18b	25.5	93	1.5	255	
20a	28	90	0	0	

[a]Estimated from crystal structure data. [b]$\Delta G_c = E(0/-1) - E(-1/-2)$ from Table 1. [c]$\Delta G_r' = 1/2[\Delta G_c - 90\ mV]$. [d]Using eq 2. [e]Using eq 3. [f]Ref 18 in Table 2 and based on $Ru_2(ap)_4$. [g]Ref 20 in Table 2.

$$\Delta G_r' = \frac{H_{ad}^2}{E_{IT}} \quad (2)$$

where E_{IT} is the intervalence band energy. We used the average energy of the lowest energy intervalence bands IT_1 in Table 2 (E_{IT} = 5400 cm^{-1}) and calculated the values of H_{ad} which were placed in Table 3.

For Class II systems, the Hush model[37] provides an alternative estimation of resonance exchange coupling using intervalence band data and eq 3.

$$H_{ad} = \frac{2.06 \times 10^{-2}}{R_{MM}}(\epsilon_{max}\nu_{max}\Delta\nu_{1/2})^{1/2} \quad (3)$$

We used the spectral data of the lowest energy intervalence transition IT_1 (Table 2) and the transition dipole moment length, R_{MM} (Table 3) in eq 3 to calculate values of resonance exchange coupling H_{ad}, which are also listed in Table 3.

In Table 3, H_{ad} derived from the free energy of comproportionation is approximately a factor of 4 greater than those calculated using the Hush model. This is not unexpected because $\Delta G_r'$ is a measure of the total thermodynamic stability of the mixed-valence complex due to metal−metal coupling. For mixed-valence complexes with more than one intervalence band, only a partial measure of the total resonance exchange can be obtained from the spectral data of a single intervalence band and eq 3. Indeed, the lower intensity of IT_1 compared to IT_2 in Table 2 must result from the poorer symmetry and energy match of metal orbitals with the orbitals of bridging μ-C_{2m} (m = 2−8) groups. The distance dependence of resonance exchange is most often described by an exponential dependence on distance:[38]

$$H_{ad} = H_0 \exp(-\gamma R) \quad (4)$$

where H_{ad} and H_0 are the donor and acceptor wave function resonance exchange at distance R and van der Waals contact, respectively, γ is a decay factor that is a measure of the medium's ability to mediate electronic coupling, and R is the separation between donor and acceptor from van der Waals contact. Assuming that R = R_{MM} (the distance separating the two nearest Ru atoms) for the mixed-valence systems $(\mathbf{4}-\mathbf{16a})^{1-}$, plots of $\ln(H_{ad})$ versus R_{MM} (Figure 5) using the two sets of H_{ad} in Table 3 yielded two linear relationships with γ = 0.12 and 0.15 $Å^{-1}$. Theory predicts a single value of γ for a

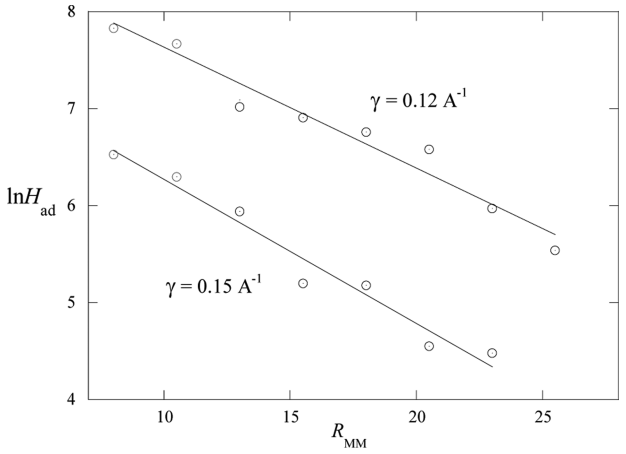

Figure 5. Distance dependence plot of $\ln(H_{ad})$ versus R_{MM} (Å) from data in Table 3. Top and bottom linear plots represent H_{ad} calculated according to eqs 2 and 3, respectively. Open circles in red are data of compounds **4** and **6a** taken from refs 18 and 20, respectively.

given bridging system or medium, and so the similarity between these two values is reassuring. The values are larger than that found for oligoene-bridged donor–acceptor pairs (0.070 $Å^{-1}$)[39] and Fc-Fc^+ donor–acceptor pairs (0.087 $Å^{-1}$),[40] but far smaller than that found for donor–acceptor pairs containing hemes (0.5–2 $Å^{-1}$)[41] or β-sheet proteins (0.9–1.15 $Å^{-1}$).[42]

DFT Study. In order to gain further understanding of the nature of electronic couplings in polyyn-diyl bridged dimer compounds, spin-unrestricted DFT calculations at the B3LYP[43]/ LanL2DZ level (Gaussian03 program)[44] were performed on the model compounds **10d** and **12d**, which correspond respectively to the compounds **10b** and **12c** with alkoxy substituents replaced by H. Most of the optimized bond lengths and angles (detailed tabulation provided in the Supporting Information) are in good agreement with the X-ray structure of **12c**. However, the optimized Ru–Ru bond distances, 2.396 Å in **10d** and 2.397 Å in **12d**, are slightly longer than the experimental value of 2.366(1) Å, which is attributed to the underestimation of weak metal–metal interactions by the DFT (B3LYP) method.[22,45] The computed energies and contour plots of the high-lying occupied MOs are given in Figure 6, and the optimized structures and geometric parameters are provided in the Supporting Information. Monoalkynyl compounds, $Ru_2(ap)_4(C_{2k}R)$, generally have three unpaired electrons originating from a $\sigma^2\pi^4\delta^2\pi^{*2}\delta^{*1}$ ground-state configuration, which has been verified from both the temperature-dependent magnetic susceptibility measurement and DFT studies.[22,46] Since the δ^* orbital is based on the Ru d_{xy} orbital, it has a minimal interaction with the $\pi(C{\equiv}C)$ orbitals due to orbital orthogonality, and the unpaired δ^* electron is localized. The π^* orbitals are composed of Ru d_{xz} and d_{yz} orbitals, which can overlap effectively with the $\pi(C{\equiv}C)$ of the axial alkynyl ligand. The π^* electrons can be delocalized onto the polyyn-diyl bridge, which is responsible for the

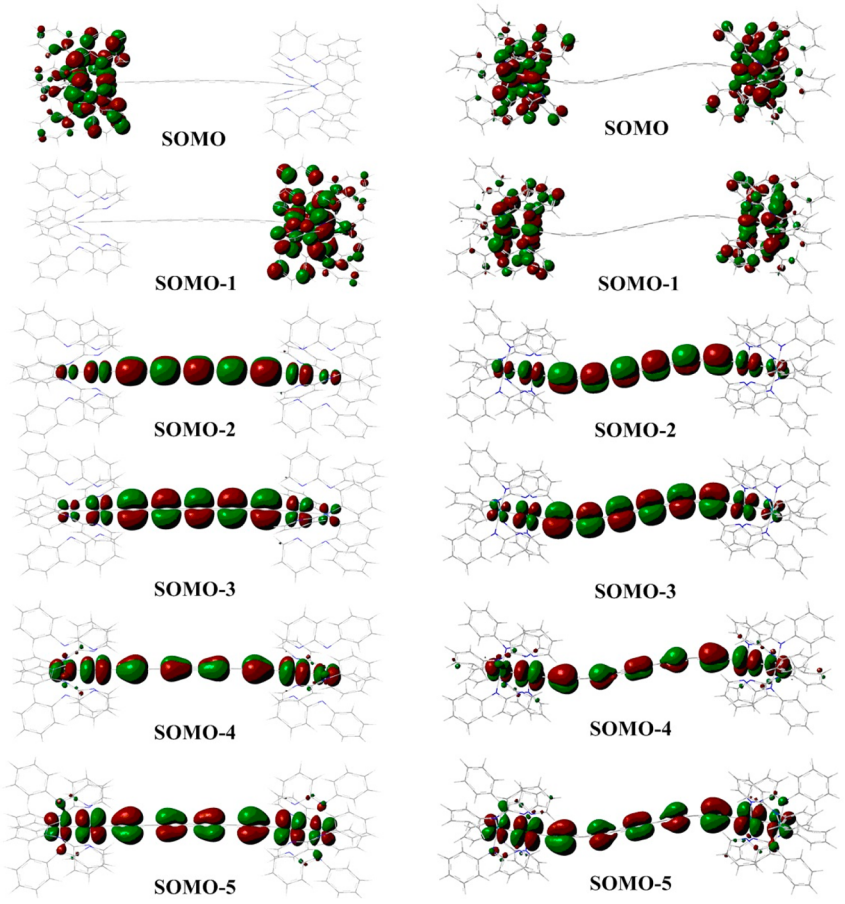

Figure 6. High-lying occupied molecular orbital diagrams for **10d** (left) and **12d** (right) obtained from DFT calculations; their energies are tabulated in the Supporting Information.

dx.doi.org/10.1021/ja507107t | J. Am. Chem. Soc. 2014, 136, 12174–12183

electronic coupling between two Ru_2 termini. Though no DFT calculations were performed on the $Ru_2(ap)_4(C_{2k}R)$ type compounds with $k > 1$, the valence orbitals of these compounds should be similar to those described for $Ru_2(ap)_4(C_2R)$.[22]

Analogous to the previous DFT study of $Ru_2(ap)_4-C_6-Ru_2(ap)_4$,[18] six magnetic (singly occupied) orbitals have been identified for each of the compounds **10d** and **12d** and depicted in Figure 6. In both cases, the SOMO and SOMO-1 are composed of the δ^*(Ru−Ru) orbitals without the contribution of the polyyn-diyl ligand. These electrons are localized on two ends of the molecule and do not contribute to the electronic coupling. Due to the weak interaction between two δ^*(Ru−Ru) orbitals, the singly occupied molecular orbitals SOMO and SOMO-1 are almost degenerate. The SOMO and SOMO-1 in **12d** appear symmetric, while those of **12d** are localized at one of the two Ru_2 ends (dissymmetric). The calculated lowest unoccupied molecular orbitals (LUMO and LUMO+1) for both **10d** and **12d** are predominantly σ(Ru−Ru)* orbitals, and their contour plots are provided in the Supporting Information.

It is clear from Figure 6 that the SOMO-2−SOMO-5 of both model compounds are primarily made of antibonding combinations of the π^*(Ru−Ru) orbitals with the π orbitals of the polyyn-diyl bridge. Clearly, the π-interaction between the Ru_2 center and axial bonded polyyn-diyl is dominated by the filled−filled type. Furthermore, both the SOMO-2 and SOMO-3 display extensive mixings between π^*(Ru−Ru) and all π(C≡C) across the C_{10} and C_{12} bridges, respectively, while the SOMO-4 and SOMO-5 have the similar bonding mode, but with less contributions from the C_{10} and C_{12} bridges.

CONCLUSION

Reported in this contribution is a comprehensive study of the series $[Ru_2(Xap)_4]_2(\mu\text{-}C_{2m})$ (m = 4−10), where the voltammetric, spectroelectrochemical, and DFT studies of an extended family of wire-like molecules revealed a persistent electronic coupling across the polyyn-diyl bridges. The calculated comproportionation constants, K_C, qualitatively revealed the class II Robin−Day mixed valency nature for $[Ru_2(Xap)_4]_2(\mu\text{-}C_{2m})$ with $m \geq 4$. The attenuation constant (γ) was found to be between 0.12 and 0.15 $Å^{-1}$ based on the electronic couplings (H_{ad}) estimated from voltammetric and spectroelectrochemical data for $[Ru_2(Xap)_4]_2(\mu\text{-}C_{2m})$ over a broad range of polyyn-diyls (m = 2−8). The spin-unrestricted DFT calculations revealed extensive mixing between the filled π^*(Ru−Ru) and π(C≡C) orbitals in the SOMO-2−SOMO-5, which are the plausible superexchange pathways between two Ru_2 termini.

EXPERIMENTAL SECTION

n-BuLi and Et_3N were purchased from Aldrich, CuCl, CuI, and *N,N,N′,N′*- tetramethylethylenediamine (TMEDA) from ACROS, and silica gel from Merck. $Ru_2(^tBuOap)_4(C_{2k}H)$,[22] $Ru_2(DiMeOap)_4(C_{2k}H)$,[21] $Ru_2(ap)_4(C_{2k}H)$ (k = 2 and 3),[30] 1,6-bistrimethylsilyl-1,3,5-hexatriyne,[47] and 1-bromo-2-triethylsilyl (BrC≡CSiEt_3)[23,24] were prepared according to literature procedures. $Ru_2(^tBuOap)_4(C_6H)$ and $Ru_2(DiMeOap)_4(C_6H)$ were synthesized by using the same method as that of $Ru_2(ap)_4(C_6H)$. The syntheses of $Ru_2(^tBuOap)_4(C_8SiEt_3)$, $Ru_2(DiMeOap)_4(C_8SiEt_3)$, $Ru_2(^tBuOap)_4(C_{10}SiEt_3)$, and $Ru_2(DiMeOap)_4(C_{10}SiEt_3)$ followed that described for $Ru_2(ap)_4(C_8SiR_3)$ and $Ru_2(ap)_4(C_{10}SiR_3)$,[30] and the details are provided in Supporting Information. THF was distilled over Na/benzophenone under an N_2 atmosphere prior to use. Unless specified, all syntheses were performed using standard Schlenk techniques under a nitrogen atmosphere. Vis-NIR spectra were acquired in THF using a JASCO V-670 UV−vis-NIR spectrophotometer. Infrared spectra were recorded on a JASCO FT/IR-ATR 6300 spectrometer. All HR-*n*ESI-MS spectra were performed on a prototype version of a QqTOF tandem mass spectrometer in CH_2Cl_2/MeOH 50/50 (Q-Star Pulsar XL; Applied Biosystems Sciex, Concord, ON, Canada). Masses were calculated by isotopic distribution utilizing Analyst 1.5 software (Applied Biosystems Sciex, Concord, ON, Canada). Both cyclic and differential pulse voltammograms were recorded in 0.20 M $(n\text{-}Bu)_4NPF_6$ solution (THF, N_2-degassed) on a CHI620A voltammetric analyzer with a glassy carbon working electrode (diameter: 2 mm), a Pt-wire auxiliary electrode, and a Ag/AgCl reference electrode. The concentration of diruthenium species is always 1.0 mM. The ferrocenium/ferrocene couple was observed at 0.575 V (vs Ag/AgCl) under experimental conditions.

General Procedure for Preparation of Dimers. (i) *Symmetric dimers*. A Schlenk tube was charged with CuCl (30 mg), acetone (20 mL), and TMEDA (2 mL) and stirred under N_2 for 0.5 h to yield a blue-green supernatant. A three-neck flask was charged with the precursor $Ru_2(Xap)_4(C_{2k}H)$ (k = 2−5, X = DiMeO or ^{t}BuO) and THF (50 mL), and dry oxygen was bubbled through with stirring for 5 min. The blue-green Cu-TMEDA supernatant was added into the three-neck flask in portions. The reaction mixture was stirred for another 0.5−2 h and then filtered through a silica gel pad (2 cm). After solvent removal, the residue was purified by a silica gel column deactivated by 10% Et_3N in hexanes using a linear gradient of eluents (THF/hexanes, 1/10 to 1/1, v/v) to give pure products. (ii) *Unsymmetric dimers*: A three-neck flask was charged with precursors $Ru_2(Xap)_4(C_{2k+2}H)$ and $Ru_2(ap)_4(C_{2k}H)$ (k = 2−4, X = DiMeO or ^{t}BuO) and 100 mL of THF, and dry oxygen was bubbled through with stirring for 5 min. The blue-green Cu-TMEDA supernatant described in (i) was added into the three-neck flask in portions. The reaction mixture was stirred for another 0.5−2 h and then filtered through a silica gel pad (2 cm). After solvent removal, the residue was purified using preparative TLC with THF/hexanes/Et_3N (1/3/0.1, v/v/v) to give pure products.

*Preparation of $[Ru_2(^tBuOap)_4]_2(\mu\text{-}C_8)$ (**8a**).* General procedure for preparation of dimers was applied using $Ru_2(^tBuOap)_4(C_4H)$ (100 mg, 0.082 mmol), and the reaction mixture was stirred for 0.5 h. Column chromatography purification afforded **8a** as a brown solid (70.9 mg, 71%). Data for **8a**: R_f (THF/hexanes = 1/2, v/v): 0.63. HR-*n*ESI-MS (m/e, based on ^{101}Ru): 2432.6893 [M^+], (calc. 2432.6901). Vis-NIR, λ_{max} (nm, ε(M^{-1} cm^{-1})): 940 (sh), 777 (10,100), 583 (10,200), 479 (14,000). IR, υ(C≡C)/cm^{-1}: 2110(w), 1940(w). Electrochemistry (THF), $E_{1/2}$/V, ΔE_p/V, $i_{forward}/i_{backward}$: 0.535, 0.130, 0.99; −0.608, 0.070, 0.79; −0.765, 0.082, 0.70; −1.741, 0.106, 0.77; −2.008, 0.068, 0.78.

*Preparation of $[Ru_2(^tBuOap)_4](\mu\text{-}C_{10})[Ru_2(ap)_4]$ (**10b**).* General procedure for preparation of dimers was applied using $Ru_2(^tBuOap)_4(C_6H)$ (100 mg, 0.081 mmol) and $Ru_2(ap)_4(C_4H)$ (75.3 mg, 0.081 mmol). The reaction mixture was stirred for 1 h. Preparative TLC purification gave **10b** as a brown solid (59.7 mg, 34%). Data for **10b**: R_f (THF/hexanes = 1/2, v/v): 0.83. HR-*n*ESI-MS (m/e, based on ^{101}Ru): 2168.4619 [M^+], (calc. 2168.4600). Vis-NIR, λ_{max} (nm, ε(M^{-1} cm^{-1})): 940 (sh), 777 (9,400), 589 (8,000), 481 (16,900). IR, υ(C≡C)/cm^{-1}: 2133(w), 2019(w), 1983(w), 1910(w). Electrochemistry (THF), $E_{1/2}$/V, ΔE_p/V, $i_{forward}/i_{backward}$: 0.548, 0.209, 0.98; −0.542, 0.130, 0.97; −0.679, 0.143, 0.92; −1.602, 0.134, 0.82; −1.859, 0.151, 1.13.

*Preparation of $[Ru_2(^tBuOap)_4]_2(\mu\text{-}C_{12})$ (**12a**).* General procedure for preparation of dimers was applied using $Ru_2(^tBuOap)_4(C_6H)$ (100 mg, 0.081 mmol), and the reaction mixture was stirred for 0.5 h. Column chromatography purification afforded **12a** as a brown solid (61.9 mg, 62%). Data for **12a**: R_f (THF/hexanes = 1/2, v/v): 0.49. HR-*n*ESI-MS (m/e, based on ^{101}Ru): 2480.6893 [M^+], (calc. 2480.6901). Vis-NIR, λ_{max} (nm, ε(M^{-1} cm^{-1})): 777 (9,400), 475 (23,000). IR, υ(C≡C)/cm^{-1}: 2116(w), 2051(w), 1933(w). Electrochemistry (THF), $E_{1/2}$/V, ΔE_p/V, $i_{forward}/i_{backward}$: 0.578, 0.113, 0.99; −0.464, 0.068, 0.96; −0.588, 0.072, 0.92; −1.463, 0.141, 0.87; −1.741, 0.116, 0.85.

*Preparation of $[Ru_2(^tBuOap)_4](\mu\text{-}C_{14})[Ru_2(ap)_4]$ (**14b**).* General procedure for preparation of dimers was applied using

$Ru_2(^tBuOap)_4(C_8H)$ (100 mg, 0.079 mmol) and $Ru_2(ap)_4(C_6H)$ (75.3 mg, 0.079 mmol). The reaction mixture was stirred for 1 h. Preparative TLC purification gave **14b** as a brown solid (49.0 mg, 28%). Data for **14b**: R_f (THF/hexanes = 1/2, v/v): 0.68. HR-*n*ESI-MS (*m*/*e*, based on ^{101}Ru): 2216.4602 [M^+], (calc. 2216.4600). Vis-NIR, λ_{max} (nm, $\varepsilon(M^{-1}\ cm^{-1})$): 780 (8,100), 418 (40,000). IR, $\upsilon(C{\equiv}C)/cm^{-1}$: 2138(w), 2082(w), 2060(w), 1957(w) and 1943(w). Electrochemistry (THF), $E_{1/2}$/V, ΔE_p/V, $i_{forward}/i_{backward}$: 0.580, 0.152, 0.98; −0.422, 0.037, 0.78; −0.536, 0.029, 0.76; −1.334, 0.121, 0.73; −1.619, 0.101, 0.82.

*Preparation of [$Ru_2(^tBuOap)_4$]$_2$(μ-C_{16}) (**16a**).* General procedure for preparation of dimers was applied using $Ru_2(^tBuOap)_4(C_8H)$ (100 mg, 0.079 mmol), and the reaction mixture was stirred for 1 h. Column chromatography purification afforded **16a** as a brown solid (55.9 mg, 56%). Data for **16a**: R_f (THF/hexanes = 1/2, v/v): 0.32. HR-*n*ESI-MS (*m*/*e*, based on ^{101}Ru): 2528.6876 [M^+], (calc. 2528.6901). Vis-NIR, λ_{max} (nm, $\varepsilon(M^{-1}\ cm^{-1})$): 778 (8,900), 432 (39,300). IR, $\upsilon(C{\equiv}C)/cm^{-1}$: 2138(w), 2073(w), 2023(m), 1932(m). Electrochemistry (THF), $E_{1/2}$/V, ΔE_p/V, $i_{forward}/i_{backward}$: 0.580, 0.074, 0.98; −0.414, 0.043, 0.91; −0.511, 0.034, 0.89; −1.220, 0.105, 0.96; −1.554, 0.052, 0.90.

*Preparation of [$Ru_2(^tBuOap)_4$](μ-C_{18})[$Ru_2(ap)_4$] (**18b**).* General procedure for preparation of dimers was applied with $Ru_2(^tBuOap)_4(C_{10}H)$ (100 mg, 0.078 mmol) and $Ru_2(ap)_4(C_8H)$ (76.2 mg, 0.078 mmol). The reaction mixture was stirred for 1 h. Preparative TLC purification gave **18b** as a brown solid (24.7 mg, 14%). Data for **18b**: R_f (THF/hexanes = 1/2, v/v): 0.48. HR-*n*ESI-MS (*m*/*e*, based on ^{101}Ru): 2264.4607 [M^+], (calc. 2264.4600). Vis-NIR, λ_{max} (nm, $\varepsilon(M^{-1}\ cm^{-1})$): 779 (10,300), 489 (30,500). IR, $\upsilon(C{\equiv}C)/cm^{-1}$: 2149(w), 2107(w), 2029(m), 1935(m), 1894(m). Electrochemistry (THF), $E_{1/2}$/V, ΔE_p/V, $i_{forward}/i_{backward}$: 0.582, 0.073, 1.03; −0.380, 0.074, 0.80; −0.473, 0.073, 0.82; −1.103, 0.073, 0.79; −1.456, 0.078, 0.77.

*Preparation of [$Ru_2(^tBuOap)_4$]$_2$(μ-C_{20}) (**20a**).* General procedure for preparation of dimers was applied with $Ru_2(^tBuOap)_4(C_{10}H)$ (100 mg, 0.078 mmol) and the reaction mixture was stirred for 1 h. Column chromatography purification afforded **20a** as a brown solid (32.2 mg, 32%). Data for **20a**: R_f (THF/hexanes = 1/2, v/v): 0.19. HR-*n*ESI-MS (*m*/*e*, based on ^{101}Ru): 2576.6898 [M^+], (calc. 2576.6901). Vis-NIR, λ_{max} (nm, $\varepsilon(M^{-1}\ cm^{-1})$): 784 (9,400), 448 (35,600). IR, $\upsilon(C{\equiv}C)/cm^{-1}$: 2154(w), 2100(w), 2037(m), 1933(m). Electrochemistry (THF), $E_{1/2}$/V, ΔE_p/V, $i_{forward}/i_{backward}$: 0.589, 0.146, 0.89; −0.340, 0.063, 0.82; −0.430, 0.055, 0.79; −0.992, 0.118, 0.78; −1.375, 0.073, 0.77.

*Preparation of [Ru_2(DiMeOap)$_4$]$_2$(μ-C_8) (**8c**).* General procedure for preparation of dimers was applied with $Ru_2(DiMeOap)_4(C_4H)$ (100 mg, 0.086 mmol) and the reaction mixture was stirred for 0.5 h. Column chromatography purification afforded **8c** as a gray solid (76.4 mg, 76%). Data for **8c**: R_f (THF/hexanes = 1/1, v/v): 0.45. HR-*n*ESI-MS (*m*/*e*, based on ^{101}Ru): 2336.3982 [M^+], (calc. 2336.3990). Vis-NIR, λ_{max} (nm, $\varepsilon(M^{-1}\ cm^{-1})$): 788 (13,800), 585 (13,200), 480 (20,600). IR, $\upsilon(C{\equiv}C)/cm^{-1}$: 2108(w), 1937(w). Electrochemistry (THF), $E_{1/2}$/V, ΔE_p/V, $i_{forward}/i_{backward}$: 0.520, 0.230, 1.11; −0.580, 0.084, 0.88; −0.758, 0.097, 0.87; −1.720, 0.131, 0.99; −1.983, 0.135, 0.92.

*Preparation of [Ru_2(DiMeOap)$_4$]$_2$(μ-C_{12}) (**12c**).* General procedure for preparation of dimers was applied using $Ru_2(DiMeOap)_4(C_6H)$ (100 mg, 0.084 mmol), and the reaction mixture was stirred for 0.5 h. Column chromatography purification afforded **12c** as a brown solid (60.1 mg, 60%). Data for **12c**: R_f (THF/hexanes = 1/1, v/v): 0.36. HR-*n*ESI-MS (*m*/*e*, based on ^{101}Ru): 2384.3996 [M^+], (calc. 2384.3990). Vis-NIR, λ_{max} (nm, $\varepsilon(M^{-1}\ cm^{-1})$): 788 (15,600), 585 (15,000), 480 (23,200). IR, $\upsilon(C{\equiv}C)/cm^{-1}$: 2115(w), 2047(w), 1932(w). Electrochemistry (THF), $E_{1/2}$/V, ΔE_p/V, $i_{forward}/i_{backward}$: 0.554, 0.090, 0.95; −0.475, 0.069, 0.92; −0.597, 0.064, 0.85; −1.453, 0.067, 1.24; −1.708, 0.067, 1.19.

*Preparation of [Ru_2(DiMeOap)$_4$]$_2$(μ-C_{16}) (**16c**).* General procedure for preparation of dimers was applied using $Ru_2(DiMeOap)_4(C_8H)$ (100 mg, 0.082 mmol), and the reaction mixture was stirred for 1 h. Column chromatography purification afforded **16c** as a brown solid (47.9 mg, 48%). Data for **16c**: R_f (THF/hexanes = 1/1, v/v): 0.25. HR-*n*ESI-MS (*m*/*e*, based on ^{101}Ru): 2432.3978 [M^+], (calc. 2432.3990). Vis-NIR, λ_{max} (nm, $\varepsilon(M^{-1}\ cm^{-1})$): 1000 (sh), 792 (12,500), 500 (sh), 436 (64,700). IR, $\upsilon(C{\equiv}C)/cm^{-1}$: 2137(w), 2073(w), 2020(m), 1929(m). Electrochemistry (THF), $E_{1/2}$/V, ΔE_p/V, $i_{forward}/i_{backward}$: 0.554, 0.087, 0.98; −0.408, 0.066, 1.16; −0.511, 0.071, 1.03; −1.206, 0.071, 1.26; −1.533, 0.076, 1.27.

*Preparation of [Ru_2(DiMeOap)$_4$]$_2$(μ-C_{20}) (**20c**).* General procedure for preparation of dimers was applied using $Ru_2(DiMeOap)_4(C_{10}H)$ (100 mg, 0.081 mmol), and the reaction mixture was stirred for 1 h. Column chromatography purification afforded **20c** as a brown solid (28.1 mg, 28%). Data for **20c**: R_f (THF/hexanes = 1/1, v/v): 0.13. HR-*n*ESI-MS (*m*/*e*, based on ^{101}Ru): 2480.3984 [M^+], (calc. 2480.3990). Vis-NIR, λ_{max} (nm, $\varepsilon(M^{-1}\ cm^{-1})$): 785 (26,700), 449 (123,000). IR, $\upsilon(C{\equiv}C)/cm^{-1}$: 2149(w), 2082(w), 2025(m), 1931-(m).Electrochemistry (THF), $E_{1/2}$/V, ΔE_p/V, $i_{forward}/i_{backward}$: 0.551, 0.073, 1.05; −0.351, 0.116, 1.33; −0.436, 0.076, 1.13; −1.001, 0.065, 1.38; −1.383, 0.061, 1.32.

X-ray Data Collection, Processing, And Structure Analysis and Refinement. Crystals of **12c** were grown via slow diffusion of ether into a dichloromethane solution of the desired compound at low temperature. A dark-red needle of compound **12c** with approximate dimensions of 0.44 × 0.19 × 0.11 mm was mounted on a glass fiber in a random orientation. The X-ray intensity data were measured on a Nonius KappaCCD diffractometer at 150 K using MoKα (λ = 0.71073 Å). The structure was solved using the structure solution program PATTY in DIRDIF99[48] and refined using the SHELX-97.[49] Crystal data of **12c**: $C_{116}H_{104}N_{16}O_{16}Ru_4$, fw = 2382.50, monoclinic, *C*2/*c*, *a* = 42.227(2), *b* = 12.433(1), *c* = 24.635(2) Å, β = 120.314(3)°, V = 11165(1) Å^3, *Z* = 4, D_{calc} = 1.417 g cm^{-3}, *R*1 = 0.082, *wR*2 = 0.201.

Computational Details. The model compound **12d** was built based on the crystal structure of **12c** with the −DiMeO groups of **12c** being replaced with −H. The model compound **10d** was also constructed based on the crystal structure of **12c** with the −DiMeO groups of **12c** being replaced with −H and one of the −C≡C− units being deleted. Full optimizations on both models have been carried out using the DFT formalism with the spin unrestricted option as implemented in the Gaussian 03 program, with the B3LYP functional. The choices of basis sets are 3-21G for H atoms, 6-31G* basis sets for C, N, O atoms, and LANL2DZ basis set for Ru atoms. In all calculations, convergence was achieved when the relative change in the density matrix between successive iterations was $<1 \times 10^{-8}$. No negative frequency was observed in the vibrational frequency analysis which indicates that these polyyn-diyl bridged Ru_2 models are metastable equilibrium structures.

Spectroelectrochemistry. An OTTLE cell was used to perform the spectroelectrochemistry. The cell had interior dimensions of roughly 1 × 2 cm with a path length of 0.2 mm and was fitted with a Ag/AgCl reference electrode and gold-foil (500 line/inch, 60% transmittance, Buckbee Mears) for the working and counter electrodes. All of the spectroelectrochemical transformations showed good reversibility (>90% recovery of original complex spectrum).

■ ASSOCIATED CONTENT

Ⓢ Supporting Information

High-resolution mass spectra of **8a**−**20a**; CVs of all monomer compounds based on ^{t}BuOap ligand, CVs and DPVs of compounds **8c**−**20c** based on DiMeOap ligand; Vis-NIR spectra of monomer compounds based on ^{t}BuOap ligand in THF; X-ray crystallographic files in CIF format for **12c**; first and second spectroelectrochemical reductions of compounds **10b**, **12a**, **14b**, and **16a**; figures of the Gaussian band fitting for compounds **10b**, **12a**, **14b**, and **16a**; equilibrium structures on model compounds **10d** and **12d**; SOMO energies of **10d** and **12d**; and full list of the authors for ref 44. This material is available free of charge via the Internet at http://pubs.acs.org.

AUTHOR INFORMATION

Corresponding Authors

tren@purdue.edu
Robert.Crutchley@carleton.ca

Author Contributions

[§]These authors contribute equally.

Notes

The authors declare no competing financial interest.

ACKNOWLEDGMENTS

We gratefully acknowledge the financial support from the National Science Foundation (CHE 1057621 and CHE 1362214) and the Purdue Research Fund to T.R., and the Natural Sciences and Engineering Research Council of Canada to R.J.C.

REFERENCES

(1) (a) Hagihara, N.; Sonogashira, K.; Takahashi, S. *Adv. Polym. Sci.* **1980**, *40*, 149. (b) Nast, R. *Coord. Chem. Rev.* **1982**, *47*, 89.

(2) (a) Hau, S. C. K.; Mak, T. C. W. *J. Am. Chem. Soc.* **2014**, *136*, 902−905. (b) Mak, T. C. W.; Zhao, X. L.; Wang, Q. M.; Guo, G. C. *Coord. Chem. Rev.* **2007**, *251*, 2311−2333.

(3) Dray, A. E.; Wittmann, F.; Friend, R. H.; Donald, A. M.; Khan, M. S.; Lewis, J.; Johnson, B. F. G. *Synth. Met.* **1991**, *41*, 871−874.

(4) (a) Chisholm, M. H. *Angew. Chem., Int. Ed.* **1991**, *30*, 673−674. (b) Bruce, M. I.; Low, P. J. *Adv. Organomet. Chem.* **2004**, *50*, 179−444. (c) Szafert, S.; Gladysz, J. A. *Chem. Rev.* **2003**, *103*, 4175−4206. (d) Szafert, S.; Gladysz, J. A. *Chem. Rev.* **2006**, *106*, 1−33. (e) Costuas, K.; Rigaut, S. *Dalton Trans.* **2011**, *40*, 5643−5658. (f) Halet, J. F.; Lapinte, C. *Coord. Chem. Rev.* **2013**, *257*, 1584−1613.

(5) Ren, T. *Organometallics* **2005**, *24*, 4854−4870.

(6) (a) Lenarvor, N.; Toupet, L.; Lapinte, C. *J. Am. Chem. Soc.* **1995**, *117*, 7129−7138. (b) Coat, F.; Paul, F.; Lapinte, C.; Toupet, L.; Costuas, K.; Halet, J.-F. *J. Organomet. Chem.* **2003**, *683*, 368−378.

(7) Zhou, Y. L.; Seyler, J. W.; Weng, W. Q.; Arif, A. M.; Gladysz, J. A. *J. Am. Chem. Soc.* **1993**, *115*, 8509−8510.

(8) Dembinski, R.; Bartik, T.; Bartik, B.; Jaeger, M.; Gladysz, J. A. *J. Am. Chem. Soc.* **2000**, *122*, 810−822.

(9) Bruce, M. I.; Low, P. J.; Costuas, K.; Halet, J. F.; Best, S. P.; Heath, G. A. *J. Am. Chem. Soc.* **2000**, *122*, 1949−1962.

(10) (a) Gao, L.-B.; Liu, S.-H.; Zhang, L.-Y.; Shi, L.-X.; Chen, Z.-N. *Organometallics* **2006**, *25*, 506−512. (b) Zhang, D.-B.; Wang, J.-Y.; Wen, H.-M.; Chen, Z.-N. *Organometallics*. **2014**, *33*, in press; http://pubs.acs.org/doi/abs/10.1021/om401235p.

(11) Kheradmandan, S.; Heinze, K.; Schmalle, H. W.; Berke, H. *Angew. Chem., Int. Ed.* **1999**, *38*, 2270−2273.

(12) Wong, K. T.; Lehn, J. M.; Peng, S. M.; Lee, G. H. *Chem. Commun.* **2000**, 2259−2260.

(13) (a) Ying, J. W.; Liu, I. P. C.; Xi, B.; Song, Y.; Campana, C.; Zuo, J. L.; Ren, T. *Angew. Chem., Int. Ed.* **2010**, *49*, 954−957. (b) Olivier, C.; Costuas, K.; Choua, S.; Maurel, V.; Turek, P.; Saillard, J.-Y.; Touchard, D.; Rigaut, S. *J. Am. Chem. Soc.* **2010**, *132*, 5638−5651. (c) Lissel, F.; Fox, T.; Blacque, O.; Polit, W.; Winter, R. F.; Venkatesan, K.; Berke, H. *J. Am. Chem. Soc.* **2013**, *135*, 3826−3833. (d) Ying, J.-W.; Cao, Z.; Campana, C.; Song, Y.; Zuo, J.-L.; Tyler, S. F.; Ren, T. *Polyhedron*. **2014**, in press; http://dx.doi.org/10.1016/j.poly.2014.05.015.

(14) (a) Schull, T. L.; Kushmerick, J. G.; Patterson, C. H.; George, C.; Moore, M. H.; Pollack, S. K.; Shashidhar, R. *J. Am. Chem. Soc.* **2003**, *125*, 3202−3203. (b) Blum, A. S.; Ren, T.; Parish, D. A.; Trammell, S. A.; Moore, M. H.; Kushmerick, J. G.; Xu, G.-L.; Deschamps, J. R.; Pollack, S. K.; Shashidhar, R. *J. Am. Chem. Soc.* **2005**, *127*, 10010−10011. (c) Mahapatro, A. K.; Ying, J.; Ren, T.; Janes, D. B. *Nano Lett.* **2008**, *8*, 2131−2136. (d) Luo, L.; Benameur, A.; Brignou, P.; Choi, S. H.; Rigaut, S.; Frisbie, C. D. *J. Phys. Chem. C* **2011**, *115*, 19955−19961. (e) Ballmann, S.; Hieringer, W.; Secker, D.; Zheng, Q.; Gladysz, J. A.; Görling, A.; Weber, H. B. *ChemPhysChem.* **2011**, *11*, 2256−2260.

(15) (a) Cotton, F. A.; Lin, C.; Murillo, C. A. *Acc. Chem. Res.* **2001**, *34*, 759−771. (b) Cotton, F. A.; Donahue, J. P.; Murillo, C. A. *J. Am. Chem. Soc.* **2003**, *125*, 5436−5450. (c) Cotton, F. A.; Donahue, J. P.; Murillo, C. A.; Perez, L. M. *J. Am. Chem. Soc.* **2003**, *125*, 5486−5492.

(16) (a) Chisholm, M. H.; Patmore, N. J. *Acc. Chem. Res.* **2007**, *40*, 19−27. (b) Chisholm, M. H.; Clark, R. J. H.; Gallucci, J.; Hadad, C. M.; Patmore, N. J. *J. Am. Chem. Soc.* **2004**, *126*, 8303−8313. Barybin, M.;. (c) Chisholm, M.; Dalal, N.; Holovics, T.; Patmore, N.; Robinson, R.; Zipse, D. *J. Am. Chem. Soc.* **2005**, *127*, 15182−15190.

(17) (a) Ren, T. *Coord. Chem. Rev.* **1998**, *175*, 43−58. (b) Ren, T.; Xu, G.-L. *Comm. Inorg. Chem.* **2002**, *23*, 355−380.

(18) Xi, B.; Liu, I. P. C.; Xu, G.-L.; Choudhuri, M. M. R.; DeRosa, M. C.; Crutchley, R. J.; Ren, T. *J. Am. Chem. Soc.* **2011**, *133*, 15094−15104.

(19) Ren, T.; Zou, G.; Alvarez, J. C. *Chem. Commun.* **2000**, 1197−1198.

(20) Xu, G.-L.; Zou, G.; Ni, Y.-H.; DeRosa, M. C.; Crutchley, R. J.; Ren, T. *J. Am. Chem. Soc.* **2003**, *125*, 10057−10065.

(21) Xi, B.; Xu, G.-L.; Ying, J.-W.; Han, H.-L.; Cordova, A.; Ren, T. *J. Organomet. Chem.* **2008**, *693*, 1656−1663.

(22) Zhang, L.; Xi, B.; Liu, I. P. C.; Choudhuri, M. M. R.; Crutchley, R. J.; Updegraff, J. B.; Protasiewicz, J. D.; Ren, T. *Inorg. Chem.* **2009**, *48*, 5187−5194.

(23) Zheng, Q.; Gladysz, J. A. *J. Am. Chem. Soc.* **2005**, *127*, 10508−10509.

(24) Zheng, Q.; Bohling, J. C.; Peters, T. B.; Frisch, A. C.; Hampel, F.; Gladysz, J. A. *Chem.—Eur. J.* **2006**, *12*, 6486−6505.

(25) Bruce, M. I.; Cole, M. L.; Ellis, B. G.; Gaudio, M.; Nicholson, B. K.; Parker, C. R.; Skelton, B. W.; White, A. H. *Polyhedron*. **2014**, http://dx.doi.org/10.1016/j.poly.2014.04.052.

(26) Antonova, A. B.; Bruce, M. I.; Ellis, B. G.; Gaudio, M.; Humphrey, P. A.; Jevric, M.; Melino, G.; Nicholson, B. K.; Perkins, G. J.; Skelton, B. W.; Stapleton, B.; White, A. H.; Zaitseva, N. N. *Chem. Commun.* **2004**, 960−961.

(27) (a) Zou, G.; Alvarez, J. C.; Ren, T. *J. Organomet. Chem.* **2000**, *596*, 152−158. (b) Xu, G.-L.; Ren, T. *Organometallics* **2001**, *20*, 2400−2404.

(28) (a) Siemsen, P.; Livingston, R. C.; Diederich, F. *Angew. Chem., Int. Ed.* **2000**, *39*, 2632−2657. (b) Mohr, W.; Stahl, J.; Hampel, F.; Gladysz, J. A. *Inorg. Chem.* **2001**, *40*, 3263−3264.

(29) Mohr, W.; Stahl, J.; Hampel, F.; Gladysz, J. A. *Chem.—Eur. J.* **2003**, *9*, 3324−3340.

(30) Xu, G. L.; Wang, C. Y.; Ni, Y. H.; Goodson, T. G.; Ren, T. *Organometallics* **2005**, *24*, 3247−3254.

(31) Meyer, W. E.; Amoroso, A. J.; Horn, C. R.; Jaeger, M.; Gladysz, J. A. *Organometallics* **2001**, *20*, 1115−1127.

(32) Geiger, W. E.; Barriere, F. *Acc. Chem. Res.* **2010**, *43*, 1030−1039.

(33) Crutchley, R. J. *Adv. Inorg. Chem.* **1994**, *41*, 273−325.

(34) (a) Stahl, J.; Mohr, W.; de Quadras, L.; Peters, T. B.; Bohling, J. C.; Martín-Alvarez, J. M.; Owen, G. R.; Hampel, F.; Gladysz, J. A. *J. Am. Chem. Soc.* **2007**, *129*, 8282−8295. (b) de Quadras, L.; Bauer, E. B.; Mohr, W.; Bohling, J. C.; Peters, T. B.; Martin-Alvarez, J. M.; Hampel, F.; Gladysz, J. A. *J. Am. Chem. Soc.* **2007**, *129*, 8296−8309.

(35) (a) Sutton, J. E.; Sutton, P. M.; Taube, H. *Inorg. Chem.* **1979**, *18*, 1017−1021. (b) Barriere, F.; Camire, N.; Geiger, W. E.; Mueller-Westerhoff, U. T.; Sanders, R. *J. Am. Chem. Soc.* **2002**, *124*, 7262−7263.

(36) Richardson, D. E.; Taube, H. *Coord. Chem. Rev.* **1984**, *60*, 107−129.

(37) Hush, N. S. *Prog. Inorg. Chem.* **1967**, *8*, 391−444.

(38) Launay, J.-P. *Chem. Soc. Rev.* **2001**, *30*, 386−397.

(39) Ribou, A. C.; Launay, J. P.; Takahashi, K.; Nihira, T.; Tarutani, S.; Spangler, C. W. *Inorg. Chem.* **1994**, *33*, 1325−1329.

(40) Ribou, A. C.; Launay, J. P.; Sachtleben, M. L.; Li, H.; Spangler, C. W. *Inorg. Chem.* **1996**, *35*, 3735−3740.

(41) Smith, D. M. A.; Rosso, K. M.; Dupuis, M.; Valiev, M.; Straatsma, T. P. *J. Phys. Chem. B* **2006**, *110*, 15582−15588.

(42) Langen, R.; Colon, J. L.; Casimiro, D. R.; Karpishin, T. B.; Winkler, J. R.; Gray, H. B. *J. Biol. Inorg. Chem.* **1996**, *1*, 221−225.
(43) (a) Becke, A. D. *J. Chem. Phys.* **1993**, *98*, 5648−5652. (b) Stephens, P. J.; Devlin, F. J.; Chabalowski, C. F.; Frisch, M. J. *J. Phys. Chem.* **1994**, *98*, 11623−11627.
(44) Frisch, M. J. et al. *Gaussian 03*, revision D.02; Gaussian, Inc.: Wallingford, CT, 2003.
(45) (a) Xu, G.-L.; Crutchley, R. J.; DeRosa, M. C.; Pan, Q.-J.; Zhang, H.-X.; Wang, X.; Ren, T. *J. Am. Chem. Soc.* **2005**, *127*, 13354−13363. (b) Liu, I. P.-C.; Ren, T. *Inorg. Chem.* **2009**, *48*, 5608−5610.
(46) Shi, Y.; Yee, G. T.; Wang, G.; Ren, T. *J. Am. Chem. Soc.* **2004**, *126*, 10552−10553.
(47) Rubin, Y.; Lin, S. S.; Knobler, C. B.; Anthony, J.; Boldi, A. M.; Diederich, F. *J. Am. Chem. Soc.* **1991**, *113*, 6943−6949.
(48) Beurskens, P. T.; Beurskens, G.; deGelder, R.; Garcia-Granda, S.; Gould, R. O.; Smits, J. M. M. *The DIRDIF2008 Program System*; Crystallography Laboratory, University of Nijmegen: The Netherlands, 2008.
(49) Sheldrick, G. M. *Acta Cryst. A* **2008**, *64*, 112.